Environmental Science Processes & Impacts

ROYAL SOCIETY OF CHEMISTRY

PAPER

Cite this: *Environ. Sci.: Processes Impacts*, 2021, **23**, 786

Photolysis of the herbicide dicamba in aqueous solutions and on corn (*Zea mays*) epicuticular waxes†

Kaitlyn Gruber, Brittany Courteau,‡ Maheemah Bokhoree, Elijah McMahon, Jenna Kotz and Amanda Nienow *

Dicamba, 3,6-dichloro-2-methoxybenzoic acid, has been used in agriculture as an herbicide for over fifty years, and has seen an increase in use in the past decade due to the development of glyphosate resistant weeds and soybeans genetically modified to resist dicamba. Despite the previous use of dicamba, many questions remain regarding its environmental fate, especially the new commercial formulations used on genetically modified crops. Here, the photolysis of dicamba, including the commercial formulation Diablo®, is examined in aqueous solutions of varying water quality and on the surface of corn epicuticular waxes. Dicamba is stable to hydrolysis but degrades under UV light. The photolytic half-life for dicamba photolysis in aqueous solutions at pH 7 irradiated with Rayonet UVB lamps (280–340 nm) was $t_{1/2}$ = 43.3 min (0.72 hours), in aqueous solutions at pH 7 in a Q-Sun solar simulator (λ > 300 nm) was $t_{1/2}$ = 13.4 hours, and on epicuticular waxes irradiated in the Q-Sun solar simulator was $t_{1/2}$ = 105 hours. Experiments with adjuvants, compounds added into the commercial formulations of dicamba, led to increases in rate constants for both aqueous and wax experiments. In addition to kinetic rate constants, photoproducts were tentatively assigned for the aqueous solution experiments. This work deepens the knowledge of the environmental fate of dicamba including the role surfactants play in chemical reactions and in providing new applications of current methods to examine the photolysis of chemicals sorbed to surfaces.

Received 1st February 2021
Accepted 9th May 2021

DOI: 10.1039/d1em00058f

rsc.li/espi

Environmental significance

In 2016, Monsanto announced Roundup Ready 2 soybeans, genetically modified soybeans that can tolerate dicamba and glyphosate. With the increased use of dicamba on soybeans, a crop to which it has not been previously applied, it has become apparent that herbicide drifting causes crop damage in adjacent fields; thus, understanding the environmental fate of dicamba is essential for maintaining ecological health. This project provides details on the environmental fate of dicamba by examining its photochemical reactivity when sorbed to epicuticular waxes, in the presence of adjuvants, and in commercial formulation. The methods used in this work can be extended to examine the photolysis of other pesticides and new pesticide formulations.

Introduction

Agrochemicals are widely used around the world. In 2012, 1182 million pounds of pesticides were used in agriculture in the United States; 678 million pounds of that amount was herbicides dedicated to the eradication of weeds.[1] For over 50 years, dicamba, 3,6-dichloro-2-methoxybenzoic acid, has been one of the agrochemicals used in the United States, historically mostly on corn or grain crops. With a pK_a of 1.87 or 1.94,[2] dicamba is a weak acid that causes death in most plants by targeting the plants' vascular tissue. Past formulations of dicamba have been listed as a restricted-use herbicide due to high potential to volatilize, leach from soils, persist in groundwater, and to cause widespread contamination of ecosystems.[3–10] The use of dicamba decreased upon the rise of glyphosate in the early 2000s, but the recent development of glyphosate resistant weeds means dicamba use is increasing again (as seen by USDA data analyzed on the Pesticide Use Data System of Hygeia Analytics).[11,12] In 2016, Monsanto announced Roundup Ready 2 soybeans, genetically modified soybeans branded under the name Xtend, that can tolerate both dicamba

Gustavus Adolphus College, 800 W College Avenue, St Peter, Minnesota 56082, USA. E-mail: anienow@gustavus.edu; Fax: +1-507-933-7041; Tel: +1-507-933-7327

† Electronic supplementary information (ESI) available: 19 first order kinetic plots showing the data used to obtain rate constants, 1 plot showing UV-Vis of dicamba in pH 7 phosphate buffer, in solutions containing NOM, and in MN River water, 1 figure showing UV-Vis of dicamba at pH 7 and pH 1 overlaid with the lamp spectra from the Rayonet and Q-Sun photoreactors, a plot showing the critical micelle concentration of MAKON DA-6, a LC-MS chromatogram, and two tables with computational data (geometries and energies). See DOI: 10.1039/d1em00058f

‡ Present address: Department of Chemistry, Iowa State University, 1605 Gilman Hall, Ames, IA 50011, USA.

and glyphosate.[13] In April 2016, the EPA allowed the use of dicamba in sprays for these soybeans for five years.[14] In July 2016, the Xtend soybeans gained EU import approval.[15] Despite conditional approval and restrictions on use, growing season 2017 saw the first use of Xtend soybeans in the US – and by the end of the summer, there were thousands of complaints from farmers with fields adjacent to those using Xtend soybeans. It has since been shown in the scientific literature that dicamba drifting is a probable cause for the crop damage in adjacent fields.[16] After lawsuits by several environmental groups, a federal circuit court revoked the EPA approval to use dicamba in June 2020; a week later, the EPA banned the sale of specific dicamba products but said farmers can spray any dicamba products already in their possession.[17] 2020 already marked the end of federal approval of dicamba products, and manufacturers would already have been submitting new applications for approval for use of the products in 2021.[18] In addition, these rulings only impact the newest formulations of dicamba product. Although the future of dicamba use in agriculture is uncertain, it is imperative to examine the chemistry of the molecule to better understand the environmental fate of the product.

Biodegradation, photodegradation, and chemical reactions are the three main pathways for eliminating pollutants from the environment. In the literature, dicamba is observed to be stable in aqueous conditions and does not undergo hydrolysis as a degradation pathway.[2] The biodegradation of dicamba has been examined in many publications.[19–22] There are a handful of papers in the literature exploring the photochemistry of dicamba, but most of the previous work on the photochemistry of dicamba has been done in aqueous solutions with advanced oxidation processes (AOP) such as the use of UV/H_2O_2 to degrade the molecule,[4] on photocatalysis processes such as using TiO_2 as a catalyst,[4,23,24] or the photo-Fenton reaction[2,25] to degrade the molecule. There has been no work investigating the photochemistry of formulated dicamba on the surface of crops or examining the role adjuvants, like those added in commercial formulations, have on the photochemistry of dicamba. Here we examine the photochemistry of dicamba in aqueous solution (without advanced oxidation processes), in solution with a model adjuvant, and on the surfaces of epicuticular waxes collected from corn plants. The photochemistry of the commercial product Diablo® was also examined in aqueous solution and on the epicuticular waxes.

Materials and methods

Chemicals and instrumentation

Analytical standards of dicamba (Sigma-Aldrich, >98.9%) were produced ranging from 0.2 mg L^{-1} to 40 mg L^{-1} in Milli-Q water (Milli-Pore). The commercial formulation of dicamba, Diablo®, was acquired from Red River Specialties, LLC and used as received. Diablo® was diluted from 480 g L^{-1} to 15 mg L^{-1} in 1 mM pH 7 phosphate buffer. Chromatographic solvents, such as acetonitrile (ACN, ≥99.9%) and water (>99.9% HPLC-grade), were purchased from Sigma-Aldrich. Phosphate buffers were prepared using H_3PO_4, $NaH_2PO_4 \cdot H_2O$, or $NaHPO_4 \cdot 3H_2O$ (Fisher Scientific) as needed in Milli-Q water and were 1 mM in total phosphate. Natural organic matter (NOM) was obtained from the International Humic Substance Society (IHSS) collected from the Suwannee River (1R101N). Actinometry solvents used were methanol (Sigma-Aldrich, ≥99.9% or EM Science, 99.97%), *p*-nitroacetophenone (Aldrich, 98%), and pyridine (Sigma-Aldrich, 99.8%). The adjuvant MAKON® DA-6 was obtained as a sample from the Stepan Company of Northfield, IL. MAKON® DA-6 is a non-ionic surfactant containing mostly isodecyl alcohol ethoxylate.

HPLC analysis for dicamba was performed using 1290 Infinity autosampler and binary pump, 1200 series thermostatted column compartment and 1100 series diode array detector (Agilent) and a reversed-phase 50 mm × 2.1 mm i.d. Eclipse Plus C18, 1.8b micron, S/N: USDAY 40893 column (Agilent). The mobile phase consisted of aqueous %A 1.7 mF phosphate buffer (pH ∼ 3) and %B ACN in a gradient of 20–50–75–20–20 %B at 0–3.5–4.0–4.01–5 minutes. A flow rate of 0.5 mL per minutes and a run time of 5 minutes were used. Sample injection volume was 20 μL, column temperature 36 °C, and UV-Vis detection set at 220 and 254 nm wavelengths. Chromatographic results from HPLC analysis for dicamba are displayed at 220 nm.

The *p*-nitroacetophenone/pyridine samples from the quantum yield experiments were analyzed in the HPLC using the same instrumentation and mobile phase. A reversed-phase 75 × 2.1 mm i.d. ACE Excel 3 Super C18, S/N: A116046 column (Advanced Chromatography Technologies LTD) was used with a gradient of 2–80–80–2–2 %B at 0–0.75–1.0–1.01–1.25 minutes. A flow rate of 0.6 mL min^{-1} was used with a stop time of 1.25 minutes, 1 μL sample injection volume, and a column temperature of 50 °C. UV-Vis detection was monitored at 288, 254, and 220 nm wavelengths. Chromatographic results from the HPLC analysis for *p*-nitroacetophenone/pyridine are displayed at 288 nm.

Photolysis of dicamba in aqueous solutions

The photolysis of dicamba was examined with three different irradiation sources: a Q-Sun Xe-1 Solar Simulator with a Daylight-Q filter, a Rayonet RPR-100 Photochemical Reactor (Southern New England Ultraviolet Company), and outdoors in St Peter, MN on the Gustavus Adolphus College campus (44° 20′ 0″ N, 93° 58′ 0″ W) in June 2019.

The photolysis of dicamba in aqueous solution (15 mg L^{-1}) with the Q-Sun Xe-1 Solar Simulator was with a Xe lamp, an irradiance of 0.40 W m^2 at 340 nm, a nominal cut-on of 295 nm, and at 30 °C. The spectral irradiance of the lamp is shown in Fig. S-21† along with the UV-Vis absorbance spectra of dicamba. Each sample of dicamba was prepared by dissolving the necessary amount of solid in phosphate buffer (at pH 7), followed by sonication for 20 minutes. 10 mL of the 15 mg L^{-1} dicamba solution was added to two glass Petri dishes which were then placed into the Q-Sun solar simulator for irradiation. Simultaneously, two Petri dishes containing PNAP/PYR actinometer were also irradiated (see details on actinometry below). Every two hours, samples were collected from the four Petri

dishes: solvent was first added back to the Petri dishes until the dishes contained 10 mL again (to account for evaporation), then 100 μL of sample was collected into HPLC vials with glass inserts and set aside for HPLC analysis. Samples were collected every two hours over four 8 hour periods with samples being stored in the refrigerator at 9 °C between the four periods.

Multiple photochemical aqueous solution reactions of dicamba (15 mg L^{-1}) were conducted using a 600 mL quartz reaction flask filled with ~500 mL dicamba, held in a Rayonet RPR-100 Photochemical Reactor (Southern New England Ultraviolet Company). Each sample of dicamba was prepared by dissolving the necessary amount of solid in desired solvent, usually phosphate buffer (at pH 7), HCl solution (pH 1), or Milli-Q water, followed by sonication for 20 minutes. In experiments with additions of adjuvant or NOM, the appropriate compound (0.24 mL of a 1.05% (w/w) MAKON® DA-6 stock to make 5 mg L^{-1} DA-6 or solid NOM to make solutions of 1 mg L^{-1}, 5 mg L^{-1}, or 10 mg L^{-1}) was added after sonication. For quenching reactions, isopropanol (final concentration of 1%) or L-histidine (final concentration of 5 mM) was added to the solution immediately prior to irradiation. In the experiment conducted with H_2O_2, 283 μL of 30% H_2O_2 was added after sonication of the 15 mg L^{-1} dicamba solution. For the experiments using Minnesota River water, river water was collected using new sample bottles that were rinsed three times before collection and then river water was filtered using a Millipore glass vacuum filter with fiber glass filter paper (5 microns). Dicamba was added to the filtered river water to make a solution of 15 mg L^{-1}. For all experiments, solutions were then added to the quartz flask for experimental irradiation in the Rayonet. Samples were irradiated in a dark room with eight 35 W low-pressure mercury lamps that emitted light centered at 310 nm. The 310 nm lamps have a spectral distribution with a full width at half max of 40 nm; the spectral irradiance of the lamps is shown in Fig. S-21.† The lamps were uniformly distributed around the vessel, and each sample was irradiated for at least 60 minutes. One set of experiments was conducted in the manner described above, but leaving the lights of the Rayonet turned off; this served as the 'dark control' to ensure any observed degradation was due to the UV-light. In addition, one set of experiments was conducted in the Rayonet with UVC lamps (254 nm) to examine the impact of wavelength.

An outdoor photolysis experiment was conducted in St Peter, MN on the Gustavus Adolphus College campus (44° 20′ 0″ N, 93° 58′ 0″ W) on June 12–13, 2019, from 11:10 am to 5:10 pm each day (samples were stored in a refrigerator overnight at 9 °C between the two days). The average temperature of a control sample (Milli-Q water) during the experimental time period was 31 ± 4 °C. 15 mL samples were placed into 14 quartz test tubes in a 4 × 6 in. black Rubbermaid notecard box at an upward angle of 45° with the open ends facing east. The irradiated samples were 15 mg L^{-1} dicamba in pH 7 phosphate buffer and 6.5×10^{-5} M PNAP/0.198 M pyridine in 50 : 50 Milli-Q water : methanol, the latter as a chemical actinometer. At hour time intervals, duplicate aliquots of 100 μL were removed and placed into amber HPLC vials. The vials were immediately stored in the refrigerator (at 9 °C) for later HPLC analysis.

Determination of dissolved oxygen concentration in aqueous dicamba solutions

A modified Winkler titration method was used to determine the dissolved oxygen (DO) concentration in oxygen rich and oxygen poor solutions in 1 mM phosphate buffer, pH ~ 7.[26] O_2 (for oxygen rich solutions) or N_2 (for oxygen poor solutions) was introduced into the solutions *via* a diffusion stone for 15 minutes before taking 1 mL samples every 10 minutes for 90 minutes (the length of one photodegradation experiment). Winkler titration solutions were made based on the literature.[26,27] Samples were added to a small test tube containing 0.5 mL of hexane. To the sample layer, 5 μL of manganese sulfate solution and 5 μL of alkali-azide-iodide solution were added consecutively and allowed to develop for 3 minutes. Concentrated sulfuric acid was added to the sample layer in 0.1 mL volume. After another 3 minutes, the sample layer was transferred to a new small test tube with 1–2 drops of starch solution (and 5 drops of Milli-Q Water for the oxygen sparged solution). The sample was titrated using a 0.000314 M sodium thiosulfate titrant. Photolysis experiments were conducted as described above with both oxygen sparged and nitrogen sparged 15 ppm dicamba solutions.

Photolysis of dicamba on corn wax surface

Corn wax trials were conducted to simulate conditions of dicamba applied onto the surface of a corn plant. The following methods were adapted from the work of ter Halle *et al.*[28] The methods have also been used by others.[29–31] For each set of experiments, approximately 160 corn plants (Anderson Seed Company, St Peter, MN) were grown in a greenhouse to the trifoliate stage, approximately 9–11 days. All corn leaves of each plant were cut off and soaked for two minutes in 75 mL of dichloromethane. The solution was then filtered with a vacuum filter and approximately 10 mL of solution was deposited onto eight glass Petri dishes and allowed to evaporate. Evaporating the solvent off left a layer of plant wax remaining on the surface of the Petri dishes. Dicamba solutions of 15 mg L^{-1} concentration were applied in 10 mL volumes and left to evaporate the solvent off, leaving a solid layer of dicamba. For the experiments with adjuvant, solutions of MAKON® DA-6 (in concentrations of 1 mg L^{-1}, 5 mg L^{-1}, 10 mg L^{-1}, or 15 mg L^{-1}) with 15 mg L^{-1} dicamba were prepared and added to the Petri dishes in the same way as above. According to dicamba field application notes, dicamba should be applied to corn at concentrations less than 0.75 lb per acre;[32] applying 10 mL of a 15 mg L^{-1} solution to a 5 mm diameter Petri dish gives a 0.68 lb per acre equivalent. Measurement of dicamba recovered from the surface prior to irradiation shows overall losses (*e.g.*, volatilization, lack of recovery, degradation in the dark, *etc.*) are less than 5%. Corn wax plates with applied dicamba samples were exposed to light (irradiance of 0.40 W m^2 at 340 nm) in a Q-Sun Xe-1 Solar Simulator with a Daylight-Q filter (nominal cut-on of 295 nm) at 42 °C. Samples were taken at time intervals ranging from 12–48 hours by reintroducing 10 mL of Milli-Q water before 1 mL aliquots were taken in duplicate. All dicamba irradiated corn wax samples were analyzed using the same HPLC parameters as

the dicamba aqueous solution samples. The same method was also used for dicamba with added adjuvant on corn wax surfaces, Diablo® on corn wax surfaces, and on dicamba on glass surfaces.

Actinometry/quantum yield of dicamba

The quantum yield of dicamba under 310 nm lamps in the Rayonet and under the Xe lamps in the Q-Sun solar simulator and in solutions of varying water quality conditions was determined using *p*-nitroacetophenone/pyridine as an actinometer. A 6.5×10^{-5} M PNAP/0.198 M pyridine solution was made in 50 : 50 Milli-Q water : methanol and was irradiated using under 310 nm lamps in the Rayonet RPR-100 photochemical reactor for 90 minutes or in the Q-Sun solar simulator for 32 hours. In the Rayonet, 1 mL aliquots were sampled in duplicate every 5 minutes and placed in amber HPLC vials. In the Q-Sun, 100 μL aliquots were sampled in quadruplicate every 1–2 hours. The samples were then analyzed in the HPLC using the methods described above. The quantum yield of dicamba was calculated from eqn (1) (adapted from Leifer eqn (6.18)):[33]

$$\phi_D = \frac{k_D}{k_{PNAP}} \left\{ \frac{\sum_\lambda \varepsilon_{\lambda,PNAP} L_\lambda}{\sum_\lambda \varepsilon_{\lambda,D} L_\lambda} \right\} \phi_{PNAP} \quad (1)$$

where k_D and k_{PNAP} are the first-order reaction rate constants for dicamba and PNAP, $\varepsilon_{\lambda,D}$ and $\varepsilon_{\lambda,PNAP}$ are the molar absorptivity (M^{-1} cm^{-1}) at each wavelength, λ, for dicamba and PNAP, L_λ is the irradiance at wavelength, λ, (einstein per cm^2 per day) and ϕ_{PNAP} is the quantum yield for PNAP ($\phi_{PNAP} = 0.0169$[pyridine]). The sums in eqn (1) were summed over wavelengths of 270–350 nm for the Rayonet 310 nm lamps and over wavelengths of 280–400 nm for the Q-Sun Xe lamps (see Fig. S-21† for spectra of the lamps). The daily-average solar irradiance spectrum for June 21 at 40° N latitude from Apell and McNeill was used to determine the quantum yield of dicamba in the outdoor experiments.[34]

Determination of environmental half-lives

The environmental half-life of dicamba was calculated using the GCSOLAR model developed by Zepp and Cline.[35] This program transforms the laboratory data collected (UV-Vis spectra of dicamba and water samples and quantum yields) into environmentally relevant half-lives. The following input parameters were used: quantum yield of dicamba in aqueous solution irradiated in the Q-Sun solar simulator, molar absorptivity coefficients of dicamba and MN River water, longitude of 94° W, clear sky, typical ozone concentration in the atmosphere, default depth parameters and water refraction index, and sea level. A series of latitudes were used as input: 30°, 40°, 50°, 60° N. The half-lives obtained were integrated over the entire day.

Preparation and analysis of dicamba photoproducts

A 40 mg L^{-1} solution of dicamba in Milli-Q water was irradiated under 310 nm lamps in the RPR-100 for 70 minutes, collecting samples every five minutes. The higher concentration and the RPR-100 were used for photoproduct analysis for analytical measurement reasons. The photoproduct separation and mass spectrometry was performed for time samples at 0, 35, and 70 minutes using an Agilent 1290 Infinity II LC coupled with an Agilent 6545XT AdvanceBio LC/Q-TOF. The mass analyzer was calibrated with a standard tuning compound mixture (Agilent, p/n: G1969-85000). The chromatographic separation was performed with a 50 mm × 2.1 mm i.d. Eclipse Plus C18, 1.8b micron, S/N: USDAY 40893 column (Agilent) with a mobile phase consisting of %A 1% formic acid in Milli-Q water, %B acetonitrile and a gradient of 2–40–75–2–2% B from 0.00–3.50–4.00–4.01–5.00 minutes. The flow rate was 0.5 mL min^{-1}, 5 μL sample injection volume, 36 °C column temperature and 50 : 50 split between the MS and DAD detector set at 254 and 220 nm wavelengths. Tandem MS was done in negative ion mode with the following electrospray ionization parameters: 4000 V capillary voltage, 2000 V nozzle voltage, 325 °C gas temperature, 5 L min^{-1} drying gas flow, 25 psig nebulizer pressure, 275 °C sheath gas temperature, and 12 L min^{-1} sheath gas flow. An 80 V fragmentor voltage for both MS dimensions was used and had a 45 V skimmer and OCT 1 FR Vpp at 750 V for the MS TOF. For both dimensions, the *m*/*z* range was 50–970 *m*/*z* with an acquisition rate of 5 spectra per s for dimension 1 and 1.5 spectra per s for dimension 2 (1152 and 3948 transients per spectrum respectively). MassHunter™ Qualitative Analysis software package, version B.08.00 (Agilent Technologies) was used to extract mass spectra from the separated photoproducts and to predict putative photoproduct molecular formulas.

Gaussian 09 (ref. 36) with WebMO graphical interface, version 17.0.012e, was used to examine the molecular energies of photoproducts, including possible isomers. All data presented are from density functional theory calculations for geometry optimization and frequency calculations using B3LYP functionals with the 6-311+G(2d,p) basis set. The default conditions of 298.15 K and 1.0 atm were used for thermochemistry calculations.

Rate constant data analysis

All reported pseudo-first-order rate constants were obtained from weighted linear least-squares analysis of the experimental data (regressing ln[*C*] *versus* time, where *C* equals the molar dicamba concentration). The weighting factors used for the regression (typically $1/\sigma_Y^2$, where σ_Y^2 is the variance on each value of ln[*C*]) were set equal to C^2 due to the transformation variable.[37] The use of this weight reduces the effect of the later time points (which are likely to have greater variance and error) on the fit of the regression line, yielding more accurate reaction rate constants. Most aqueous experiments were conducted in at least duplicate, and Table 1 lists the number of trials for each set of experiments, *n*. The standard deviations for experiments in Table 1 with $n \geq 2$ are the standard deviations over the trials, and the standard deviations for experiments with $n = 1$ is the standard deviation of the regression fit (used as an approximation as a true standard deviation was unable to be calculated).

Table 1 Rate constants for dicamba photodegradation and number of trials for each experiment, *n*

Conditions	*k*/per day	*n*
254 nm lamps, pH 7	56.2 ± 2.9	1
No UV-light	No reaction	1
310 nm lamps, pH 7	23.0 ± 2.9	6
310 nm lamps, pH 1	20.2 ± 1.4	2
310 nm lamps, O_2 sat'd	21.6 ± 4.3	2
310 nm lamps, N_2 sat'd	58 ± 29	2
310 nm lamps, Diablo®	21.6 ± 1.4	3
310 nm lamps, 5 mg L^{-1} DA6	33.1 ± 7.2	2
310 nm lamps, 5 mg L^{-1} DA6, IPA	24.5 ± 5.8	2
310 nm lamps, 5 mg L^{-1} DA6, histidine	20.2 ± 2.9	1
310 nm lamps, 5 mM H_2O_2	93.6 ± 2.9	1
Outdoors, July 2019, Saint Peter, MN	0.04 ± 0.03	1
Q-Sun Xe lamps, pH 7	1.3 ± 0.7	2
Glass plate	No reaction	1
Corn wax	0.16 ± 0.01	1
Corn wax/Diablo®	0.30 ± 0.03	1
Corn wax/1 mg L^{-1} DA-6	0.26 ± 0.03	1
Corn wax/5 mg L^{-1} DA-6	0.32 ± 0.03	1
Corn wax/10 mg L^{-1} DA-6	0.19 ± 0.03	1
Corn wax/15 mg L^{-1} DA-6	0.22 ± 0.01	1

Results and discussion

Aqueous experiments

Kinetics of dicamba photolysis. The UV-Vis spectra of dicamba as a function of irradiation time is shown in Fig. 1. As can be seen in the figure, the absorbance peak near 203 nm, corresponding to dicamba, decreases with increasing irradiation time. There is an isosbestic point near 235 nm formed between the decreasing dicamba peak and the increasing peak with a center near 254 nm.

Each photolysis reaction of dicamba examined showed an exponential decrease of dicamba, suggesting that the photodegradation follows a first order or pseudo first order reaction mechanism. Fig. 2 shows a selection of the photolysis data, illustrating the first order nature of the reaction. The figure shows a photolysis experiment (conditions: 15 mg L^{-1} dicamba buffered with 1 mM phosphate buffer at pH 7, irradiated with 310 nm light in the Rayonet) and an experiment conducted in the dark (conditions: 15 mg L^{-1} dicamba buffered with 1 mM phosphate buffer at pH 7, with no irradiation). The dark control experiment showed no loss of dicamba over 70 minutes and confirmed that dicamba was not lost *via* evaporation in the aqueous solution photoreaction chamber. The photolysis experiments of dicamba, applying 310 nm irradiation to a 15 mg L^{-1} solution of dicamba buffered to pH 7, in a quartz photoreaction flask (experiment conducted $n = 6$ times), yielded a photodegradation rate constant of $k = 23.0 \pm 2.9$ per day. Also illustrated in Fig. 2 are the kinetic data plots for two additional experiments: irradiation of dicamba in the Rayonet photoreactor with (a) an oxygen desaturated solution and (b) with addition of 5 mM H_2O_2. These two reactions will be discussed further below. These four rate constants can be found in Table 1, a summary of all rate constants from this work. The ESI contains all the plots (S1–S19)† used to obtain the aqueous rate constants in Table 1.

Table 1 also provides the rate constants for the experiments completed with aqueous solutions in the Q-Sun solar simulator

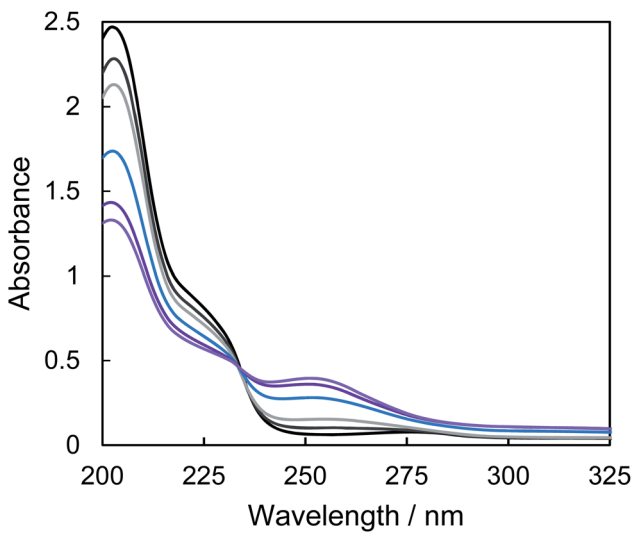

Fig. 1 A selection of UV-Vis spectra of dicamba irradiated at 310 nm. Looking at 200 nm, the top black line is non-irradiated dicamba and bottom purple line is dicamba irradiated for 55 min. The lines in between were irradiated from 5–50 minutes. The peak at 203 nm corresponds to dicamba; absorbance at that wavelength drops over the irradiation time. Another peak at 254 nm grows in over the irradiation time. An isosbestic point can be seen near 235 nm.

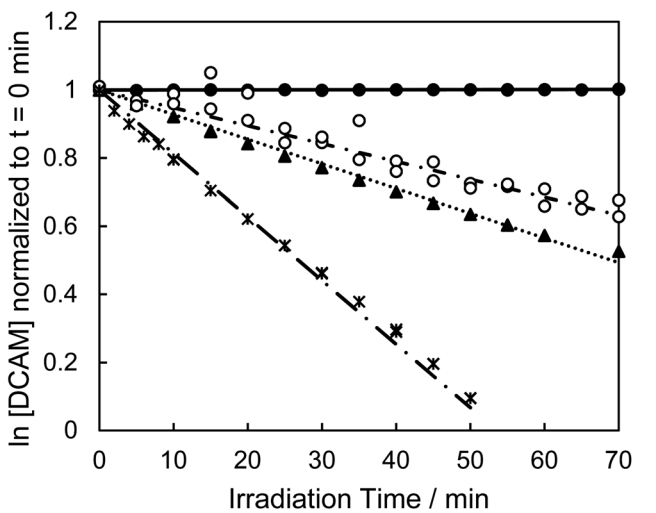

Fig. 2 15 mg L^{-1} at pH 7 dicamba kept the dark (●) and irradiated under 310 nm lamps (▲). Regression lines yield no reaction for the dark control and $k = 23.0 \pm 2.0$ per day for the irradiated sample. Also shown are 15 mg L^{-1} at pH 7 dicamba irradiated under 310 nm lamps in oxygen desaturated solution (○) and with 5 mM H_2O_2 (*). Regression lines give $k = 58 \pm 29$ per day for the experiment with oxygen desaturated solution and 93.6 ± 2.9 per day for the 5 mM H_2O_2 experiment. These rate constants show the decrease in rate due to the removal of oxygen in the oxygen desaturated solution and the increase in rate due to reaction with hydroxyl radial in the H_2O_2 experiment.

($k = 1.3 \pm 0.7$ per day) and outdoors in June 2019 ($k = 0.04 \pm 0.03$ per day). These two experiments also had an exponential decrease of dicamba over irradiation time, but the reaction rates are much slower than those for the reactions conducted in the Rayonet. The slower rate is presumably due to the spectra of light from the two light sources: both the Q-Sun solar simulator and the sun have a cut-off at 295 nm which limits exposure to some of the higher energy wavelengths present in the Rayonet. The quantum yield for dicamba at pH 7 irradiated in the Q-Sun was determined to be 0.0013, and the quantum yield for dicamba outdoors was 0.0012. These quantum yields, which are calculated relative to photon flux from each light source, are nearly identical, showing that the Q-Sun solar simulator is a good lab based light source to use to examine the environmental fate of dicamba.

Dicamba photolysis in varied pH and wavelength

The impact of wavelength on the photodegradation of dicamba was examined in the Rayonet reactor by using both UVC (254 nm) and UVB (280–340 nm, centered at 310 nm) lamps. The observed rate constant for the photodegradation of dicamba under 254 nm light was 56.2 ± 2.9 per day (Fig. S2†). This rate constant is a factor of 2 larger than the rate constant obtained under the 310 nm lamps, and two orders of magnitude larger than the reaction in the Q-Sun. The difference in degradation observed with the different lamps is due to differences in photon flux and energy of the photons from the two sets of lamps, the differences in absorbance of light by dicamba at the two wavelengths, and possibly due to different reaction mechanisms. Since UVC light is not environmentally relevant, no further work was done at this wavelength. Although the Rayonet UVB light source is not a perfect model for environmental light sources, the Rayonet UVB light was used for a series of further experiments to more deeply explore the photochemistry of dicamba as these experiments could be conducted more quickly than experiments outdoors or in the Q-Sun solar simulator, allowing time for more exploration of the photochemical reactions. In addition, a quick look at the irradiated samples from the Q-Sun on the LC-MS showed similar photoproducts to the samples from the samples irradiated with the Rayonet UVB lamps, suggesting that the mechanisms may be similar.

The pKa of dicamba has been observed to be about 1.9, and the molecule is primarily deprotonated at a pH of 7.[2] Despite the fact that dicamba will be in the carboxylate form in natural waters, there may be environmental circumstances where the protonated form may be important. Therefore, experiments of dicamba photolysis in aqueous solutions were conducted under UVB light in the Rayonet in HCl solutions at pH 1. A rate constant of 20.2 ± 1.4 per day was observed, suggesting that the reaction is slightly slower in acidic conditions than in the solutions at pH 7. Although the absorbance of 310 nm light is similar for the solutions buffered at both pH 1 and pH 7 (see Fig. S-21†), the quantum yield of the protonated form of dicamba ($\phi = 0.048$) is lower than that of the deprotonated form ($\phi = 0.073$) which leads to the observed slowing of the reaction under acidic conditions. Thus, the slower reaction at pH 1 is due almost entirely due to the lower quantum yield for the protonated form. The favoring of photodegradation in the anionic form has also been observed for other herbicides with a benzoic acid moiety.[38,39] The quantum yields obtained here can also be compared to that obtained by Aguer *et al.*; these authors obtained a quantum yield of 0.022 for the deprotonated form of dicamba at a wavelength of 275 nm.[2] Aguer *et al.* also observed that the absorbance of acidic solutions of dicamba was greater than the absorbance of basic/neutral solutions as is shown from this work in Fig. S-21.† Although the wavelengths used in the two studies (this one and the one by Aguer *et al.*) differ slightly, the quantum yields are found to be on the same order of magnitude. However, both the quantum yields from the Rayonet experiment and the Aguer *et al.* paper are an order of magnitude larger than the quantum yields obtained from the Q-Sun and outdoor experiments due to the wavelengths of light used in each experiment. For environmental purposes, the quantum yield from the Q-Sun and/or outdoor experiment should be used.

Environmental direct photolysis half-lives of dicamba

Using the quantum yield of dicamba at pH 7 under the Xe lamp of the Q-Sun solar simulator (*i.e.*, $\phi = 0.0013$), the GCSOLAR model was used to determine the environmental direct photolysis half-lives dependent on the season and the degree of latitude in pure water and in Minnesota River water. These direct photolysis half-lives are presented in Table 2. As seen in the table, the half-lives for dicamba range from 3.74 to 97.7 days under these conditions. As expected, half-lives are longer in the winter months and at higher latitudes. Overall, this analysis suggests that dicamba will photodegrade in the environment within days in the typical growing season (summer) and crop

Table 2 Environmental direct photolysis half-lives of dicamba calculated from GCSOLAR

		Integrated half-life (days)	
Season	Latitude (°)	DCAM in MN River water	DCAM in Milli-Q water
Spring	30	4.23	4.23
	40	4.68	4.68
	50	5.48	5.48
	60	6.83	6.83
Summer	30	3.74	3.74
	40	3.84	3.84
	50	4.08	4.08
	60	4.49	4.49
Fall	30	6.13	6.13
	40	8.21	8.21
	50	12.8	12.8
	60	25.5	25.5
Winter	30	8.63	8.63
	40	14.2	14.2
	50	30.3	30.3
	60	97.7	97.7

locations (latitudes 35°–45° N) in the United States. These half-lives are on the same order of magnitude as those reported for degradation in aerobic soil in the EPA registration for dicamba.[40]

Dicamba photolysis in varied oxygen concentration

Photodegradation experiments were conducted in oxygen sparged and nitrogen sparged solutions under UVB light in the Rayonet to further examine the role of oxygen in the photodegradation of dicamba. The average dissolved oxygen content in the oxygen sparged solution was 13 ± 4 mg L^{-1} with no significant drop in dissolved oxygen content over the 90 minutes. The average dissolved oxygen content in the nitrogen sparged solution was 2.8 ± 0.8 mg L^{-1} with no significant change in dissolved oxygen content over the 90 minutes; this corresponds to approximately 1/5th of the dissolved oxygen in the oxygen sparged solution. It was assumed that the addition of 15 mg L^{-1} of dicamba would not alter the dissolved oxygen concentration in the buffered solutions, and Winkler titrations were not repeated with dicamba containing aqueous solutions prior to the photolysis.

The photodegradation rate constant in the nitrogen sparged solution was determined to be 58 ± 29 per day, a factor of three greater than that of the photodegradation rate constant in the oxygen sparged experiment (21.6 ± 4.3 per day). The kinetic data from the nitrogen sparged solution can be seen in Fig. 2. The inhibiting effect of oxygen has also been observed in the photolysis of 5-halogenosalicylic acids,[41] compounds with structural similarities to dicamba, and in the photolysis of chlorothalonil.[42] Using laser flash photolysis and computational chemistry calculations, the authors of the paper on halogenosalicylic acids were able to show that oxygen quenched the triplet excited state of the acids.[41] Given the structural similarities of dicamba to these acids, it is hypothesized that the triplet excited state of dicamba is important in its photochemistry and that oxygen acts as a quencher of this state. At reduced oxygen levels, the lifetime of the triplet is longer, leading to faster photoreactions.

Diablo® and adjuvants

The rate constant of Diablo® photodegradation in aqueous solution under UVB light in the Rayonet, 21.6 ± 1.4 per day, was statistically consistent with the rates seen with aqueous solution experiments of dicamba (Table 1). This is not necessarily intuitive as the additional ingredients in the commercial mix could interact with the dicamba and/or the light to lead to a different reaction rate and/or mechanism.

As discussed in the introduction, one category of molecules added to commercial herbicides mixtures are adjuvants, designed to help the solutions spread on surfaces. A series of experiments were conducted to explore the impact of these adjuvants on the photodegradation of dicamba. The concentrations and types of adjuvants used in commercial forms of dicamba are proprietary, but there are several surfactants available on the market. Here, a solution of 5 mg L^{-1} MAKON® DA-6, an isodecyl alcohol ethoxylate, and 15 mg L^{-1} dicamba was tested to model a commercial formulation in solution. The rate constant for the model commercial formulation, 33.1 ± 7.2 per day, was significantly higher than the aqueous solution experiments of dicamba.

Several papers in the literature have found that nonionic surfactant molecules can photosensitize organic molecules such as herbicides.[43–50] The photosensitization of the dicamba photolysis in the solutions with DA-6 could be due to micelle formation changing the environment in solution, from energy transfer between the herbicide and surfactant, and/or indirect photolysis from the formation of other reactive species. Micelles can form in solutions with surfactant if the concentration of surfactant is above the critical micelle concentration (cmc). For Makon DA-6, an isodecyl alcohol ethoxylate with 6 ethoxylate units, the cmc is estimated to be above 400 ppm.[51] For the experiments presented here, with 5 ppm DA-6, no micelles should be formed. Experiments verifying this conclusion are described in the ESI.† Micelles, therefore, should not be the reason for the enhanced photodegradation. No experiments were conducted to test the hypothesis that energy transfer may be leading to the photosensitization, but this has been observed in the literature on photochemistry and nonionic surfactants.[45–48]

To investigate whether the adjuvant was contributing to an indirect photolysis pathway, quenchers for singlet oxygen (5 mM L-histidine) and hydroxyl radical (1% isopropanol) were separately added to solutions of adjuvant/dicamba and irradiated. The rate constants for the indirect photolysis experiments of 15 mg L^{-1} dicamba with 5 mg L^{-1} DA-6 using L-histidine and isopropanol as quenchers were 20.2 ± 2.9 per day and 24.5 ± 5.8 per day respectively (Table 1). These photodegradation rate constants are consistent with the direct photodegradation rate constant of dicamba, suggesting that there may be indirect photolysis occurring in these solutions. It remains unclear what reactive species may be forming in these reactions, and how

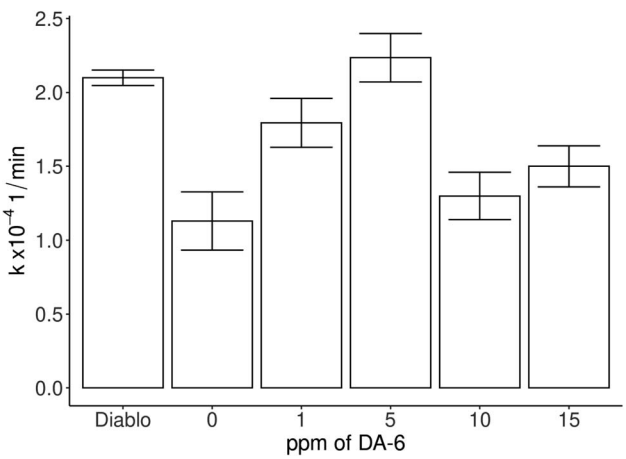

Fig. 3 Photodegradation rate constants of dicamba the surfaces of corn wax. Included are: photodegradation rate constant of Diablo®, a commercial product of dicamba, on the surface of corn wax and photodegradation rate constants of dicamba on the surface of corn wax surfaces with 0 ppm adjuvant DA-6, 1 ppm DA-6, 5 ppm DA-6, 10 ppm DA-6, and 15 ppm DA-6.

they are formed, but it is known that dicamba will react with hydroxyl radicals (the literature gives rate constant for the reaction of dicamba with hydroxyl radical as either $k_{OH} = 1.3 \times 10^9\ M^{-1}\ s^{-1}$ or $3.5 \times 10^9\ M^{-1}\ s^{-1}$ at pH 7 and $T = 20\ ^\circ C$).[52,53] We also conducted an experiment examining the susceptibility of dicamba to hydroxyl radical reactions by irradiating a 15 mg L^{-1} dicamba solution spiked with 5 mM H_2O_2. When irradiated at 310 nm, H_2O_2 can produce hydroxyl radicals (quantum yield for this reaction at 308 nm is 1.93 ± 0.39).[54] As can be seen in Table 1 and in Fig. 2, the photodegradation rate constant for dicamba in the H_2O_2 spiked experiment was 93.6 ± 2.9 per day, indicating that dicamba photodegradation rates are much faster in the presence of hydroxyl radicals. Although the H_2O_2 experiment illustrates that dicamba can react with hydroxyl radicals, it does not provide evidence that hydroxyl radicals are involved in the experiments with the surfactant DA-6. Overall, it has proven challenging to conclude exactly why the surfactant experiments show an increase in photodegradation rate.

Dicamba photolysis in varied natural organic matter (NOM) concentration

Natural organic matter (NOM) is found in all river waters, commonly at concentrations between 1 and 10 mg L^{-1}.[55] The structure and chemical composition of NOM varies due to soil type, location, biological degradation, and other factors. In these experiments, Suwannee River NOM, ordered from the International Humic Substances Society, was used as a model NOM. This NOM largely consists of C (52.47% by mass), O (42.69% by mass), H (4.19% by mass), and N (1.10% by mass) and should be negatively charged at pH values of 6–9 due to carboxylic acid functional groups. It has been shown by previous groups that the presence of NOM in water samples can either increase[56–58] or decrease.[38,58–62]photodegradation rates. The increase in reaction rates is attributed to the ability of NOM to produce reactive oxygen species such as hydroxyl radicals and/or triplet NOM, and the decrease in rates is typically attributed to screening of light by the NOM.

As can be observed in Table 3, and Fig. S-16,† an inverse relationship between NOM concentrations and degradation rates of dicamba was observed in NOM/dicamba experiments. The addition of 1.2 mg L^{-1} NOM to 15 mg L^{-1} of dicamba caused no change in reaction ($k = 23.0 \pm 1.4$ per day); adding 5.2 mg L^{-1} of NOM to 15 mg L^{-1} dicamba slowed the reaction down and yielded rate constant of 15.8 ± 1.4 per day; and adding 10.0 mg L^{-1} of NOM to 15 mg L^{-1} dicamba yielded a rate constant of 13.0 ± 1.4 per day. These reaction rate constants suggest that there is no measurable photosensitization, but it may be likely that light screening is occurring. To test for the latter, the screening models presented in Leifer's "*The Kinetics of Environmental Aquatic Photochemistry: Theory and Practice*" book and in Schwarzenbach, Gschwend, and Imboden's *Environmental Organic Chemistry* book, were used to correct the measured rate constants for screening:

$$S(\lambda) = \frac{1 - 10^{-D(\lambda)\alpha(\lambda)z_{mix}}}{2.3 z_{mix} D(\lambda)\alpha(\lambda)} \quad (2)$$

where $S(\lambda)$ is the screening factor, $D(\lambda)$ is the distribution function (equal to 1 in these experiments), z_{mix} is the vertical distance in a mixed body of water (equal to 4.6 cm in these experiments), and $\alpha(\lambda)$ is the attenuation coefficient of the medium.[33,58] $\alpha(\lambda)$ was obtained from UV-Vis spectra of NOM and dicamba solutions, similar to the work of Espy, *et al.*[38] Because the lamps used in the Rayonet photoreactor have a narrow wavelength range, the photodegradation rate constants obtained in the presence of NOM can be corrected for light screening by dividing the rate constants by the screening factor:

$$k_{corr} \approx \frac{k_{obs}^{NOM}}{S(\lambda)} \quad (3)$$

where k_{obs}^{NOM} is the experimental degradation rate constant for dicamba in the presence of NOM and k_{corr} is the photodegradation rate constant corrected for light screening. Using the equations above, the observed rate constants from the NOM experiments were corrected to account for screening. The corrected rate constants are given in Table 3. As can be seen in the table, the corrected rate constants match (within experimental error) the photodegradation rate constant of dicamba in buffered solution. This shows that the observed decrease in photodegradation rate upon the addition of NOM is accounted for by screening effects.

Since the experiments with Suwannee River NOM suggested that screening may be an important factor in natural water systems, Minnesota River water was collected and used as a matrix for photodegradation experiments in the lab. The Minnesota River water was collected in St Peter, MN in June 2019 and June 2020, and was filtered using a Millipore filtering system prior to spiking the water with dicamba to a concentration of 15 mg L^{-1}. Although the Minnesota River water was not analyzed, the soil in this area of Minnesota is mostly Lester soil, known to be a loamy soil with nearly equal amounts of sand and

Table 3 Experimental (k_{obs}) and light screening corrected (k_{corr}) rate constants for irradiation of pH 7 dicamba. $z_{mix} = 4.6$ cm and $D(\lambda) = 1$ in calculations of $S(\lambda)$

Solution	k_{obs} (per day)	$S(\lambda)$	k_{corr} (per day)
Dicamba	23.0 ± 1.4		
Dicamba + 1.2 mg L^{-1} NOM	23.0 ± 1.4	0.958	23.0 ± 1.4
Dicamba + 5.2 mg L^{-1} NOM	15.8 ± 1.4	0.756	21.6 ± 1.4
Dicamba + 10.0 mg L^{-1} NOM	13.0 ± 1.4	0.619	23.0 ± 1.4
Dicamba in MN river water – 2019	8.9 ± 1.4	0.580	15.8 ± 1.4
Dicamba in MN river water – 2020	14.4 ± 1.4	0.884	15.8 ± 1.4

silt, slightly lower clay amounts, and soil organic matter in the range of 2–5%.[63] The rate constant from these experiments, along with the screening factor, and corrected rate constant are available in Table 3. The rate constants obtained from these experiments show that photodegradation of dicamba in natural waters is slower than any of the photodegradation experiments with Suwannee River NOM. Although there is a slight difference between the samples collected from the two different years, the absorbance of light by the Minnesota River water is much stronger than in any of the experiments with Suwannee River NOM, and the calculated screening factor for the Minnesota River water is 0.580 in 2019 and 0.884 in 2020. From the 2019 value, one would predict screening is more prevalent in that Minnesota River sample as compared to the lab experiments with Suwannee River NOM. However, when the rate constant is corrected using the screening factor, the corrected rate constant is still slower than the photodegradation rate constant of dicamba in buffered solution. The same is observed with the 2020 sample. Hence, screening alone does not account for the observed drop in photodegradation rate constant of dicamba in the Minnesota River water.

Adsorption of dicamba to a component in the Minnesota River water is a possibility to explain the slower reaction rate in the experiments with the Minnesota River water. Several authors have examined the sorption of dicamba to soils.[64,65] Sakaliene *et al.*, found the adsorption coefficient of dicamba to be the lowest for the series of herbicides they examined, with a K_d value ranging from 0.03–0.08 L kg^{-1} depending on the soil type. These low K_d values suggest that adsorption is not likely to be the reason for the observed slower reaction rate. This is supported by the fact that dicamba and the NOM are both negatively charged at the pH levels in these experiments, and it has been shown that negatively charged organic species will adsorb more weakly than the related neutral compound to anionic NOM.[58] In addition, areas of the HPLC peaks from the non-irradiated wax samples align with the non-applied solutions, suggesting no adsorption occurs upon application. Thus, it remains unclear what is causing the reduced photodegradation rate constant of dicamba in the Minnesota River water experiments.

Photolysis on epicuticular corn wax

Recent studies suggest that the matrix environment in which photolysis studies are conducted can affect both photochemical transformation rates and the photoproduct composition.[66–70] For example, the epicuticular wax of most species absorbs light below 350 nm and also contains photosensitizing functional groups such as carboxyl groups.[71–73] Thus, in comparison to photolysis in water samples or other appropriate controls, photolysis of pesticides sorbed to epicuticular wax can be slower (*e.g.*, due to light screening or phase) or faster (*e.g.*, due to photosensitization).

The experiments with corn waxes are inherently difficult and lengthy due to the time needed to grow the corn, extract and plate the epicuticular wax, and complete the irradiation (so one set of experiments is typically 23–25 days). Dicamba was applied to the surface and irradiated as a solid. Four different sets of corn plants were grown to test the degradation of dicamba on the surface of the waxes. The average rate constant for the photodegradation of dicamba on the surface of corn wax was 0.16 ± 0.01 per day. The rate constants observed on the corn wax surfaces a factor of ~9 slower than the rate constant from the aqueous solution experiment conducted in the Q-Sun solar simulator, and can be attributed to the solid state of the dicamba during irradiation.

For comparison, an experiment where dicamba was irradiated after deposition directly on the glass Petri dishes was conducted. Other groups interested in the surface photochemistry of herbicides have also used glass or quartz as a comparison.[2,29,30,66,69] The experiments with dicamba directly deposited on the glass Petri dishes yielded no statistically significant reaction. This result can be compared to that of Aguer *et al.* who found that the photolysis rate constant of dicamba was greater when deposited on clay surfaces compared to the photolysis rate when dicamba was deposited on glass.[2] In contrast, the herbicides isoproturon and 2,4-D (and related chlorinated phenoxyacetic acids herbicides) and the plant activator acibenzolar *S*-methyl were found to react faster on glass surfaces than on paraffin wax.[29,30,66,69] The corn wax used here may have a surface more similar to the clay surfaces used by Aguer compared to paraffin wax surfaces. On the corn waxes, there may be better dispersion across the surface as compared to the glass (perhaps in part because dicamba is anionic in the solid state and glass surfaces are negatively charged).[2] In addition, Aguer *et al.* found that dicamba is in a microcrystalline form when in the solid state.[2] Photolysis in this state is likely slower because less surface is exposed to light and screening can be expected for the central part of the microcrystals. We speculate that the corn wax might allow the dicamba to spread more evenly across the surface.

Herbicides are generally applied in the field as formulations including the active ingredient and various adjuvants. The most important class of adjuvants is surfactants, used to reduce the surface tension of the spray solution in the field, allowing droplets to spread on the foliage. Today, the most commonly used surfactants used are alkyl ethoxylated surfactants.[74] A series of experiments were conducted to examine the impact adding adjuvant to the epicuticular wax surfaces has on the photodegradation of dicamba. A surfactant, MAKON® DA-6 (Stepan Company) was added to the surface at several concentrations: 1 mg L^{-1}, 5 mg L^{-1}, 10 mg L^{-1} and 15 mg L^{-1} (yielding surface concentrations of 5.1×10^{-4} mg cm^{-2}, 2.6×10^{-3} mg cm^{-2}, 5.1×10^{-3} mg cm^{-2}, and 7.7×10^{-3} mg cm^{-2} respectively). Table 1 shows the rate constants from these experiments alongside the rate constant from the experiment without adjuvant. Adding adjuvant to the experiment increased the photodegradation rate constant; with 1 mg L^{-1} DA-6, the rate constant increased to 0.26 ± 0.03 per day and with 5 mg L^{-1} DA-6, the rate constant increased to 0.32 ± 0.03 per day (Fig. 3). This increase is likely due to the adjuvant breaking apart pesticide aggregates as observed by other authors.[69] However, at higher concentrations of DA-6, the rate constant drops again. We believe this is due to experimental limitations; at

Table 4 Data from the LC-MS for each putative photoproduct of the photolysis of dicamba (40 mg L^{-1}) irradiated at 310 nm for 0, 35, and 70 min

Photoproduct	Proposed putative photoproduct structure	Measured mass ESI $[M - H]^-$ m/z	Calculated $[M - H]^-$ m/z	Error (ppm)	Formula	DBE	RT/min
Dicamba	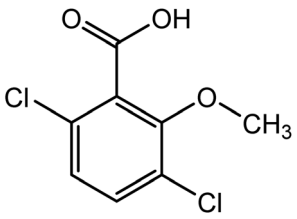	218.9629	218.9616	−2.66	$C_8H_6Cl_2O_3$	5	3.227
A	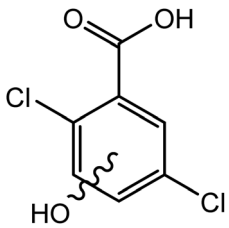	204.9464	204.9459	0.09	$C_7H_4Cl_2O_3$	5	2.915
B		186.9806	186.9798	−0.73	$C_7H_5ClO_4$	5	2.737
B1 – top	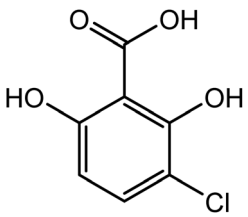						
B2 – bottom	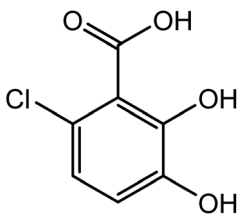						
C		234.9572	234.9565	−0.7	$C_8H_6Cl_2O_4$	5	2.109
C1 – top	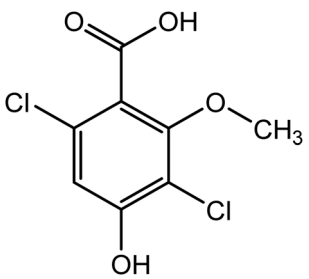						
C2 – bottom	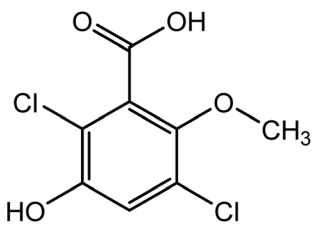						

Table 4 (*Contd.*)

Photoproduct	Proposed putative photoproduct structure	Measured mass ESI $[M-H]^-$ m/z	Calculated $[M-H]^-$ m/z	Error (ppm)	Formula	DBE	RT/min
D		200.9964	200.9955	−1.45	$C_8H_7ClO_4$	5	1.919
D1 – top	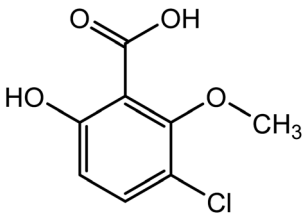						
D2 – bottom	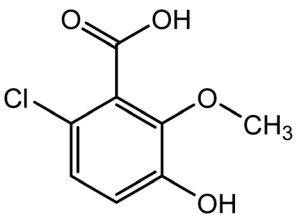						
E	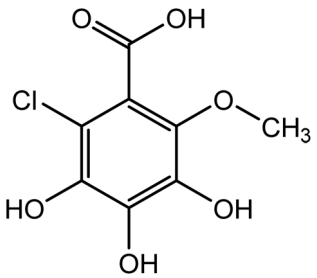	232.9864	232.9853	−2.0	$C_8H_7ClO_6$	5	0.809
F	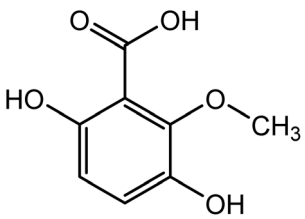	183.0301	183.0294	−1.05	$C_8H_8O_5$	5	1.795

concentrations of DA-6 above 5 mg L^{-1}, the corn wax layer starts to physically degrade (visibly detaching from the Petri dish and breaking apart), and some dicamba and DA-6 may be present underneath the wax layer rather than at the surface. The corn wax layer also degraded with 15 mg L^{-1} DA-6, but the rate constant appears higher than the experiment with 10 mg L^{-1} DA-6; since the degradation of the wax was not controlled, perhaps more dicamba remained on the surface in the 15 mg L^{-1} experiment. Also shown in Table 1 and Fig. 3 is an experiment where the commercial product Diablo® was applied to the surface of corn wax. As with the adjuvant experiments, an increase in photodegradation was observed, suggesting that there are other ingredients in the commercial products that lead to faster photodegradation on the wax surfaces. Due to the complexity of these experiments, the photoproducts and degradation pathways of the reaction on the surface of the epicuticular waxes has not been examined.

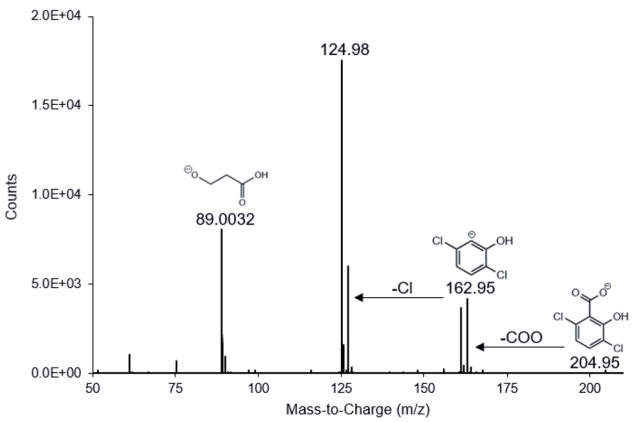

Fig. 4 2D MS of photoproduct A, 204.9461 m/z parent ion peak. The fragmentation pattern of the parent peak ion, 204.9461 m/z, indicates the presence the carboxylic acid group due to the 162.95 m/z fragment. The presence of two chlorine atoms was determined from the mass difference and isomer patterns between 124.98 m/z and 162.95 m/z fragments.

Photoproduct analysis

Putative photoproducts were determined using LC-MS-MS analysis of dicamba samples irradiated in aqueous solution under UVB light in the Rayonet at times 0, 35, and 70 minutes. The putative photoproduct structures, measured mass, calculated mass, error, and formula are summarized in Table 4. Proposed structures were determined through fragmentation patterns of tandem mass spectra. The chromatogram collected from the LC-MS is shown in Fig. S-23† and a summary of the computational work related to photoproducts is presented in Tables S-2 and S-3.† These photoproduct assignments would be at Level 3: Tentative Candidates on the Schymanski scale.[75]

The structure of photoproduct A was tentatively assigned through the 2D MS fragmentation pattern of the peak ion 204.9461 *m*/*z* with 162.9534 *m*/*z* and 124.9797 *m*/*z* peak fragments indicating loss of a carboxylic acid group and a chlorine atom respectively (Fig. 4). Photoproduct A has a 0.09 ppm error calculated for the measured mass, calculated mass, and chemical formula. The 1D MS chlorine splitting pattern and a calculated 5 double bond equivalence confirmed continued presence of the aromatic ring and carboxylic acid as well as both chlorine atoms. This putative photoproduct shows a loss of a methoxy group and gain of an alcohol group. There is no direct evidence of where the alcohol group adds to the ring, but DFT calculations using B3LYP/6-311+G(2d,p) show that the isomer with the alcohol group meta to the carboxylic acid is 2.20 kcal mol^{-1} lower in energy than the isomer with the alcohol group para to the carboxylic acid, and 6.96 kcal mol^{-1} lower in

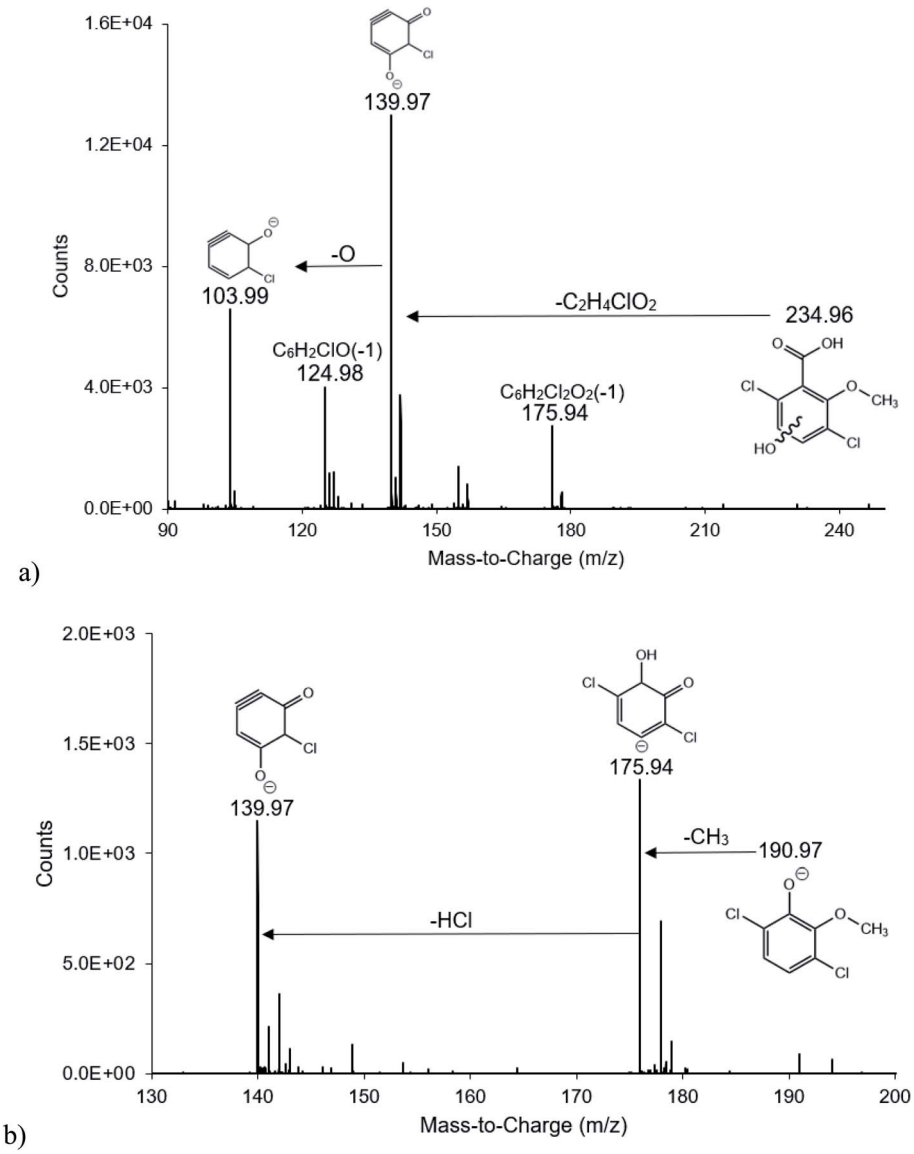

Fig. 5 2D MS of photoproduct C, 234.9564 *m*/*z* parent peak ion and 190.9668 *m*/*z* base peak ion. (a) Fragmentation patterns in the 2D MS of the parent peak ion 234.9564 *m*/*z* suggest the presence of a carboxylic acid group, two chlorine atoms, and the ether and alcohol groups meta or para from each other. (b) The fragmentation pattern in the 2D MS of the base peak ion 190.9668 *m*/*z* confirms two chlorine atoms, an ether group from the 175.94 *m*/*z* peak, and an alcohol group.

energy than the isomer with the alcohol group ortho carboxylic acid. This product has also been observed in work examining the photochemistry of dicamba in the presence of TiO_2.[4,23]

The structure of photoproduct B was tentatively assigned using the 1D MS Cl splitting pattern, 5 double bond equivalence and the evidence of dimerization within the MS after ESI ionization, all suggesting that the carboxylic acid remained on the ring. The −0.73 error of the measured mass compared to the calculated mass and molecular formula is strong evidence that photoproduct B is an addition of an alcohol group in replacement of a chlorine atom, and replacement of the methyl ether group with an alcohol group. Time dependent DFT calculations using B3LYP/6-311+G(2d,p) showed that the chlorine–carbon bond meta to the carboxylic acid had a larger change in bond length upon excitation. DFT calculations were also used to determine the molecular energy of three possible isomers of this putative photoproduct (differing by where on the ring the two alcohol groups are attached). Two of these isomers are shown in Table 4; isomer B1, with the two alcohol groups ortho to the carboxylic acid, had the lowest energy of the three isomers examined, and is 1.17 kcal mol^{-1} lower in energy than photoproduct B2. This photoproduct has also been observed by Fabbri *et al.* in their work with TiO_2 induce photochemistry of dicamba; these authors also show the product in the form of photoproduct B1.[4]

The structure of photoproduct C was tentatively assigned using the 2D MS fragmentation pattern of peak ions 234.9564 *m*/*z* and 190.9668 *m*/*z*. The 5 double bond equivalence suggests that the carboxylic acid group remains in addition to the ring, and the isomer pattern shows that both chlorines are still attached. Fig. 5a shows the 2D MS fragmentation pattern of the 234.9564 *m*/*z* parent peak ion which indicates the presence of a carboxylic acid group from the 175.94 *m*/*z* peak, and two chlorine atoms from the isomer pattern seen in all fragments. The alcohol and ether group were determined from the 175.94 *m*/*z* and 139.97 *m*/*z* fragments (Fig. 5a and b). The 2D MS

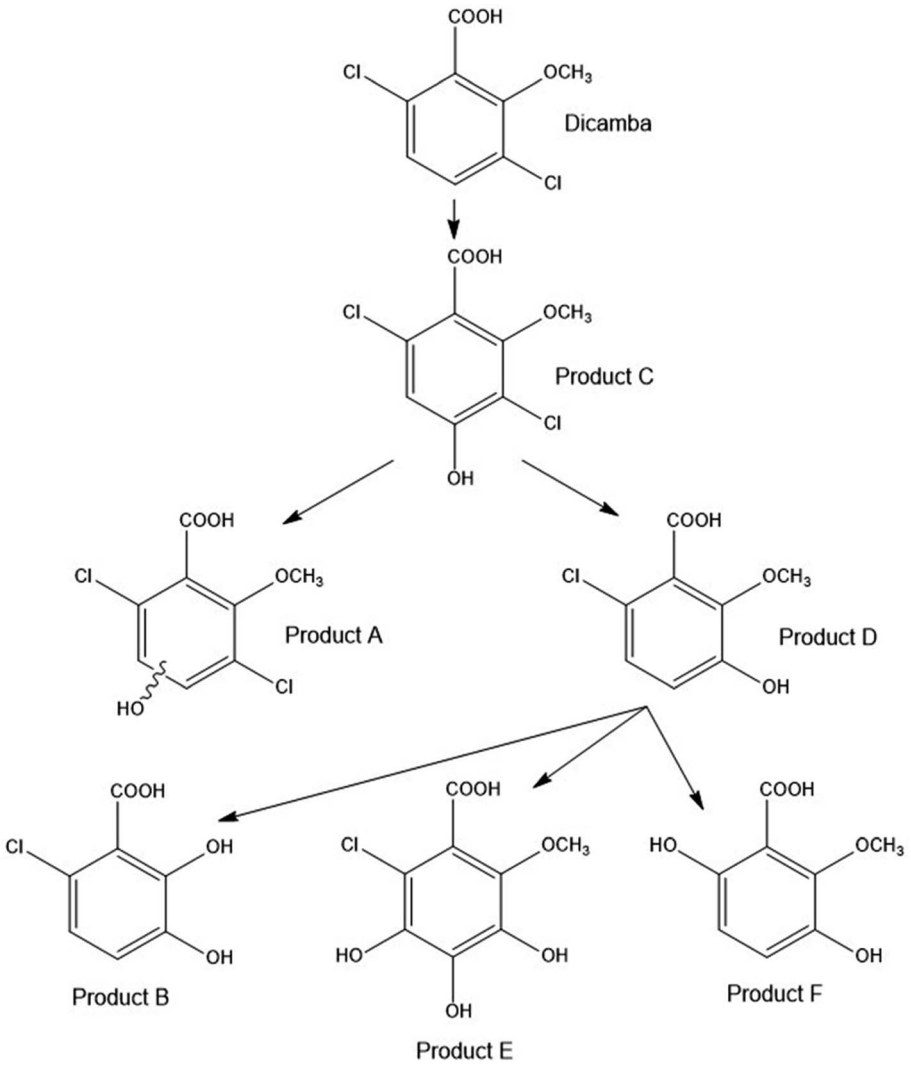

Fig. 6 Proposed transformation pathway of photodegradation of dicamba. Proposed transformation pathway was determined from LC-MS-MS data and the similar transformation pathway presented in Fabbri *et al.*[4] Isomers with the lowest energy as determined by DFT calculations are shown in the proposed transformation pathway.

fragmentation pattern of the 190.9668 *m*/*z* peak ion confirmed the two chlorine atoms from the isomer pattern visible in all fragments, the loss of an ether group from the 175.94 *m*/*z* peak, and the loss of an alcohol group from the 139.97 *m*/*z* peak (Fig. 5b). DFT calculations were again used to determine the energetic stability of possible isomers of this photoproduct. Isomer C1, with the alcohol group para to the carboxylic acid was found to be 0.21 kcal mol^{-1} lower in energy than isomer C2.

The structure of photoproduct D was tentatively assigned through use of the fragmentation pattern of the 1D MS with fragment 157.0064 *m*/*z* signaling the loss of the carboxylic acid. The 2D MS of the 200.9958 *m*/*z* peak ion showed a fragmentation pattern of the loss of the methyl group from the methyl ether and a subsequent loss of the chlorine from peaks 141.9824 *m*/*z* and 107.0078 *m*/*z* subsequently. Thus, we can conclude that the photoproduct contains one chlorine atom, a carboxylic acid group, and a methoxy group. The 5 double bond equivalence and the evidence of dimerization within the MS also show that the carboxylic acid remains on this photoproduct. Time dependent DFT calculations using B3LYP/6-311+G(2d,p) were also completed with photoproduct D, and again the chlorine–carbon bond meta to the carboxylic acid had a larger change in bond length upon excitation. DFT calculations also show that isomer D2 is 1.25 kcal mol^{-1} lower in energy than D1. Both pieces of computational evidence support that the chlorine meta to the carboxylic acid is the chlorine that has been lost during the formation of this photoproduct. This product has been observed in work examining the photochemistry of dicamba in the presence of TiO_2 but both papers do not assign a location for the alcohol group and chlorine atom.[4,23]

The structure of photoproduct E was tentatively assigned using 2D MS of the peak ion 232.9865 *m*/*z* and the fragmentation pattern suggesting the loss of the carboxylic acid (173.9715 *m*/*z*), the loss of a chlorine atom and methyl group (137.9960 *m*/*z*), and the loss of an oxygen (125.0238 *m*/*z*). Fabbri *et al.* also observed this photoproduct in their work with the photodegradation of dicamba in the presence of TiO_2.[4]

The structure of photoproduct F was tentatively assigned from 1D MS by the lack of a chlorine splitting pattern, and the 153.0194 *m*/*z* fragment that specified the loss of a carboxylic acid group. The presence of the carboxylic acid group was confirmed by the calculated 5 double bond equivalence. We draw the putative photoproduct with the two alcohol groups taking the place of the missing two chlorine atoms. This is another photoproduct also observed in the work of Fabbri *et al.*[4] and it has also been observed by Aguer *et al.*[2] Both of the photoproducts observed in the irradiation of dicamba in aqueous solution in the Aguer paper had a double substitution of chlorine for two alcohol groups; perhaps the singly substituted photoproducts were not observed due to the experimental conditions/irradiation time.[2]

Fig. 6 shows a proposed transformation pathway for the photodegradation of dicamba in aqueous solution. This proposed transformation pathway is similar to that presented by Fabbri *et al.* for the photolytic degradation of dicamba in UV–TiO_2 and UV–H_2O_2 processes,[4] and is supported by our LC-MS-MS data and putative photoproduct assignments. In the transformation pathway, the first photoproduct formed is photoproduct C, the addition of an alcohol group to dicamba. As with Fabbri,[4] we posit two different photoproducts forming from photoproduct C–photoproduct A, which is a loss of the methoxy group from dicamba, and photoproduct D, loss of one chlorine and the addition of an alcohol group at the position meta to the carboxylic acid. This isomer of photoproduct D is illustrated as it was found to have the lowest energy in the DFT calculations. From photoproduct D, photoproducts B, E, and F form. These photoproducts illustrate further loss of chlorine and addition of alcohol groups to the ring. Photoproduct B also has a loss of the methoxy group on dicamba. Unlike Fabbri *et al.*, we see no further photoproducts/steps in the proposed transformation pathway. We also saw no evidence for the oxidation of the methoxy group Fabbri *et al.* included in their scheme.[4] We may not be observing these photoproducts due to the different experimental conditions, analytical capabilities, and/or the reaction times that were examined.

Conclusion

This project provides details on the environmental fate of dicamba, showing that while the molecule is stable in water and does not undergo hydrolysis, it is susceptible to photolysis when in aqueous solution, on epicuticular waxes, in the presence of surfactants, and in formulation. The quantum yield of dicamba, along with the GCSOLAR program, shows that the environmental half-life of the compound is on the order of days, especially in the spring and summer months in which dicamba is applied to fields. The addition of adjuvants causes an increase in photodegradation of dicamba both in aqueous solution and on epicuticular waxes of corn. Experiments saturating the solutions with nitrogen gas show that the presence of oxygen quenches the photodegradation, suggesting that the triplet excited state of dicamba is involved in the photochemistry. Analysis of photoproducts showed an evolution of aromatic compounds.

Funding source

This work has been funded by National Science Foundation Grant #1808276.

Author contributions

Kaitlyn Gruber: data curation, formal analysis, methodology, validation, investigation, visualization, supervision, writing – original draft, writing – review & editing; Brittany Courteau: data curation, formal analysis, methodology, validation, investigation, visualization, funding acquisition, supervision, writing – original draft, writing – review & editing; Maheemah Bokhoree: formal analysis, validation, investigation, visualization, writing – original draft, writing – review & editing; Elijah McMahon: formal analysis, investigation, writing – original draft; Jenna Kotz: formal analysis, investigation, writing – original draft; Amanda Nienow: conceptualization, data curation, funding acquisition, formal analysis, investigation, methodology,

project administration, resources, supervision, validation, visualization, writing – original draft, writing – review & editing.

Conflicts of interest

There are no conflicts to declare.

Acknowledgements

This research was funded by the National Science Foundation Grant #1808276 and Gustavus Adolphus College. We extend our gratitude to Dr Dwight Stoll, Dr Gabriel Leme, and Hayley Lhotka for their help with gathering chromatographic spectra and mass spectra.

References

1 D. Atwood and C. Paisley-Jones, *Pesticides Industry Sales and Usage: 2008–2012 Market Estimates*, U.S. Environmental Protection Agency.
2 J.-P. Aguer, F. Blachère, P. Boule, S. Garaudee and C. Guillard, Photolysis of dicamba (3,6-dichloro-2-methoxybenzoic acid) in aqueous solution and dispersed on solid supports, *Int. J. Photoenergy*, 2000, **2**, 81–86, DOI: 10.1016/S1010-6030(02)00238-1.
3 W. Chu and C. C. Wong, The photocatalytic degradation of dicamba in TiO2 suspensions with the help of hydrogen peroxide by different near UV irradiations, *Water Res.*, 2004, **38**, 1037–1043, DOI: 10.1016/j.watres.2003.10.037.
4 D. Fabbri, A. B. Prevot and E. Pramauro, Analytical monitoring of the photo-induced degradation of 3,6-dichloro-2-methoxybenzoic acid in homogeneous and heterogeneous systems, *Res. Chem. Intermed.*, 2007, **33**, 393–405, DOI: 10.1163/156856707779238694.
5 R. Behrens and W. E. Lueschen, Dicamba Volatility, *Weed Sci.*, 1979, **27**, 486–493.
6 J. F. Egan and D. A. Mortensen, Quantifying vapor drift of dicamba herbicides applied to soybean, *Environ. Toxicol. Chem.*, 2012, **31**, 1023–1031, DOI: 10.1002/etc.1778.
7 T. C. Mueller, D. R. Wright and K. M. Remund, Effect of Formulation and Application Time of Day on Detecting Dicamba in the Air under Field Conditions, *Weed Sci.*, 2013, **61**, 586–593, DOI: 10.1614/WS-D-12-00178.1.
8 S. D. Strachan, M. S. Casini, K. M. Heldreth, J. A. Scocas, S. J. Nissen, B. Bukun, R. B. Lindenmayer, D. L. Shaner, P. Westra and G. Brunk, Vapor Movement of Synthetic Auxin Herbicides: Aminocyclopyrachlor, Aminocyclopyrachlor-Methyl Ester, Dicamba, and Aminopyralid, *Weed Sci.*, 2010, **58**, 103–108, DOI: 10.1614/WS-D-09-00011.1.
9 S. D. Strachan, N. M. Ferry and T. L. Cooper, Vapor Movement of Aminocyclopyrachlor, Aminopyralid, and Dicamba in the Field, *Weed Technol.*, 2013, **27**, 143–155, DOI: 10.1614/WT-D-12-00096.1.
10 J. R. Baur and R. W. Bovey, Ultraviolet and volatility loss of herbicides, *Arch. Environ. Contam. Toxicol.*, 1974, **2**, 275–288.
11 USDA NASS, https://quickstats.nass.usda.gov/, accessed 17 December 2020.
12 *Pesticide Use Data System*, https://hygeia-analytics.com/tools/puds/by-crop/, accessed 17 December 2020.
13 *Roundup Ready 2 Xtend Soybeans: Currently in Phase IV of Monsanto's R&D Pipeline*, Monsanto.
14 B. E. Erickson, *Chem. Eng. News*, 2016, **94**, 15.
15 *Roundup Ready 2 Xtend Soybeans Gain EU Import Approval*, Monsanto, St Louis, MO, 2016.
16 H. Hatterman-Valenti, G. Endres, B. Jenks, M. Ostlie, T. Reinhardt, A. Robinson, J. Stenger and R. Zollinger, Defining Glyphosate and Dicamba Drift Injury to Dry Edible Pea, Dry Edible Bean, and Potato, *HortTechnology*, 2017, **27**, 502–509, DOI: 10.21273/HORTTECH03679-17.
17 D. Charles, Court Ruling on Popular Weedkiller Dicamba Upends Midwestern Agriculture, *Morning Edition*, National Public Radio, 2020.
18 S. Tong, *Marketplace*, National Public Radio, 2020.
19 A. M. Fogarty and O. H. Tuovinen, Microbiological degradation of the herbicide dicamba, *J. Ind. Microbiol.*, 1995, **14**, 365–370, DOI: 10.1007/BF01569952.
20 J. P. Krueger, R. G. Butz and D. J. Cork, Aerobic and anaerobic soil metabolism of dicamba, *J. Agric. Food Chem.*, 1991, **39**, 995–999, DOI: 10.1021/jf00005a039.
21 E. W. Pavel, A. R. Lopez, D. F. Berry, E. P. Smith, R. B. Reneau and S. Mostaghimi, Anaerobic degradation of dicamba and metribuzin in riparian wetland soils, *Water Res.*, 1999, **33**, 87–94, DOI: 10.1016/S0043-1354(98)00181-X.
22 P. W. Milligan and M. M. Häggblom, Biodegradation and Biotransformation of Dicamba under Different Reducing Conditions, *Environ. Sci. Technol.*, 1999, **33**, 1224–1229, DOI: 10.1021/es981117e.
23 M. A. Rahman and M. Muneer, Heterogeneous Photocatalytic Degradation of Picloram, Dicamba, and Floumeturon in Aqueous Suspensions of Titanium Dioxide, *J. Environ. Sci. Health, Part B*, 2005, **40**, 247–267, DOI: 10.1081/PFC-200045546.
24 A. Bianco-Prevot, D. Fabbri, E. Pramauro, A. Morales-Rubio and M. de la Guardia, Continuous monitoring of photocatalytic treatments by flow injection. Degradation of dicamba in aqueous TiO_2 dispersions, *Chemosphere*, 2001, **44**, 249–255, DOI: 10.1016/S0045-6535(00)00168-5.
25 E. Brillas, M. Á. Baños and J. A. Garrido, Mineralization of herbicide 3,6-dichloro-2-methoxybenzoic acid in aqueous medium by anodic oxidation, electro-Fenton and photoelectro-Fenton, *Electrochim. Acta*, 2003, **48**, 1697–1705, DOI: 10.1016/S0013-4686(03)00142-7.
26 A. Shriwastav, G. Sudarsan, P. Bose and V. Tare, Modification of Winkler's method for determination of dissolved oxygen concentration in small sample volumes, *Anal. Methods*, 2010, **2**, 1618, DOI: 10.1039/c0ay00110d.
27 A. D. Eaton, M. A. H. Franson, L. S. Clesceri, E. W. Rice and A. E. Greenberg, 4500-O C: Azide Modification, In *Standard Methods For the Examination of Water and Wastewater*, American Public Health Association, Washington, D.C., 21st edn, 2005, p. 4:138:1404:–:1404:4:140.

28 A. ter Halle, D. Drncova and C. Richard, Phototransformation of the herbicide sulcotrione on maize cuticular wax, *Environ. Sci. Technol.*, 2006, **40**, 2989–2995, DOI: 10.1021/es052266h.

29 P. P. Choudhury, Leaf cuticle-assisted phototransformation of isoproturon, *Acta Physiol. Plant.*, 2017, **39**(8), DOI: 10.1007/s11738-017-2471-0.

30 P. Choudhury, Leaf-cutin assisted phototransformation of 2,4-D ethyl ester, *Indian J. Biochem. Biophys.*, 2016, **53**, 227–231.

31 S. C. Anderson, A. Christiansen, A. Peterson, L. Beukelman and A. M. Nienow, Statistical analysis of the photodegradation of imazethapyr on the surface of extracted soybean (*Glycine max*) and corn (*Zea mays*) epicuticular waxes, *Environ. Sci.: Processes Impacts*, 2016, **18**, 1305–1315, DOI: 10.1039/C6EM00401F.

32 *Dicamba Herbicide Application Notes*, Drexel Chemical Company.

33 A. Leifer, *The Kinetics of Environmental Aquatic Photochemistry: Theory and Practice*, American Chemical Society, 1988.

34 J. N. Apell and K. McNeill, Updated and validated solar irradiance reference spectra for estimating environmental photodegradation rates, *Environ. Sci.: Processes Impacts*, 2019, **21**, 427–437, DOI: 10.1039/C8EM00478A.

35 R. G. Zepp and D. M. Cline, Rates of direct photolysis in aquatic environment, *Environ. Sci. Technol.*, 1977, **11**, 359–366, DOI: 10.1021/es60127a013.

36 M. J. Frisch, G. W. Trucks, H. B. Schlegel, G. E. Scuseria, M. A. Robb, J. R. Cheeseman, G. Scalmani, V. Barone, B. Mennucci, G. A. Petersson, H. Nakatsuji, M. Caricato, X. Li, H. P. Hratchian, A. F. Izmaylov, J. Bloino, G. Zheng, J. L. Sonnenberg, M. Hada, M. Ehara, K. Toyota, R. Fukuda, J. Hasegawa, M. Ishida, T. Nakajima, Y. Honda, O. Kitao, H. Nakai, T. Vreven, J. A. Montgomery Jr, J. E. Peralta, F. Ogliaro, M. Bearpark, J. J. Heyd, E. Brothers, K. N. Kudin, V. N. Staroverov, R. Kobayashi, J. Normand, K. Raghavachari, A. Rendell, J. C. Burant, S. S. Iyengar, J. Tomasi, M. Cossi, N. Rega, J. M. Millam, M. Klene, J. E. Knox, J. B. Cross, V. Bakken, C. Adamo, J. Jaramillo, R. Gomperts, R. E. Stratmann, O. Yazyev, A. J. Austin, R. Cammi, C. Pomelli, J. W. Ochterski, R. L. Martin, K. Morokuma, V. G. Zakrzewski, G. A. Voth, P. Salvador, J. J. Dannenberg, S. Dapprich, A. D. Daniels, Ö. Farkas, J. B. Foresman, J. V. Ortiz, J. Cioslowski and D. J. Fox, *Gaussian 09*, Gaussian, Inc., Wallingford, CT, 2009.

37 J. R. Green and D. Margerison, *Statistical Treatment of Experimental Data*, Elsevier Scientific Publishing Company, New York, 1977.

38 R. Espy, E. Pelton, A. Opseth, J. Kasprisin and A. M. Nienow, Photodegradation of the Herbicide Imazethapyr in Aqueous Solution: Effects of Wavelength, pH, and Natural Organic Matter (NOM) and Analysis of Photoproducts, *J. Agric. Food Chem.*, 2011, **59**, 7277–7285, DOI: 10.1021/Jf200573g.

39 H. Barkani, C. Catastini, C. Emmelin, M. Sarakha, A. El Azzouzi and J. M. Chovelon, Study of the phototransformation of imazaquin in aqueous solution: a kinetic approach, *J. Photochem. Photobiol., A*, 2005, **170**, 27–35, DOI: 10.1016/j.jphotochem.2004.07.017.

40 D. Edwards, *Reregistration Eligibility Decision for Dicamba and Associated Salts*, United States Environmental Protection Agency.

41 R. Tafer, P. de Sainte-Claire, P. Vicendo, A. Boulkamh and C. Richard, Photochemistry of 5-Halogenosalicylic Acids: Evidence of the Triplet Involvement in the Carbene Formation, *ChemistrySelect*, 2016, **1**, 4704–4712, DOI: 10.1002/slct.201600979.

42 H. He, D. Xiong, F. Han, Z. Xu, B. Huang and X. Pan, Dissolved oxygen inhibits the promotion of chlorothalonil photodegradation mediated by humic acid, *J. Photochem. Photobiol., A*, 2018, **360**, 289–297, DOI: 10.1016/j.jphotochem.2018.04.050.

43 F. S. Tanaka, R. G. Wien and E. R. Mansager, Effect of nonionic surfactants on the photochemistry of 3-(4-chlorophenyl)-1,1-dimethylurea in aqueous solution, *J. Agric. Food Chem.*, 1979, **27**, 774–779, DOI: 10.1021/jf60224a016.

44 F. S. Tanaka, R. G. Wien and E. R. Mansager, Survey for surfactant effects on the photodegradation of herbicides in aqueous media, *J. Agric. Food Chem.*, 1981, **29**, 227–230, DOI: 10.1021/jf00104a005.

45 F. S. Tanaka, R. G. Wien and B. L. Hoffer, Photosensitized degradation of a homogeneous nonionic surfactant: hexaethoxylated 2,6,8-trimethyl-4-nonanol, *J. Agric. Food Chem.*, 1986, **34**, 547–551, DOI: 10.1021/jf00069a045.

46 W. Chu and C. T. Jafvert, Photodechlorination of Polychlorobenzene Congeners in Surfactant Micelle Solutions, *Environ. Sci. Technol.*, 1994, **28**, 2415–2422, DOI: 10.1021/es00062a029.

47 F. S. Tanaka, R. G. Wien and R. G. Zaylskie, Photolytic degradation of a homogeneous Triton X nonionic surfactant: nonaethoxylated *p*-(1,1,3,3-tetramethylbutyl) phenol, *J. Agric. Food Chem.*, 1991, **39**, 2046–2052, DOI: 10.1021/jf00011a033.

48 Z. Shi, M. E. Sigman, M. M. Ghosh and R. Dabestani, Photolysis of 2-Chlorophenol Dissolved in Surfactant Solutions, *Environ. Sci. Technol.*, 1997, **31**, 3581–3587, DOI: 10.1021/es9703279.

49 K. Huang, G. Lu, Z. Zheng, R. Wang, T. Tang, X. Tao, R. Cai, Z. Dang, P. Wu and H. Yin, Photodegradation of 2,4,4′-tribrominated diphenyl ether in various surfactant solutions: kinetics, mechanisms and intermediates, *Environ. Sci.: Processes Impacts*, 2018, **20**, 806–812, DOI: 10.1039/C8EM00033F.

50 X. Li, J. Huang, G. Yu and S. Deng, Photodestruction of BDE-99 in micellar solutions of nonionic surfactants of Brij 35 and Brij 58, *Chemosphere*, 2010, **78**, 752–759, DOI: 10.1016/j.chemosphere.2009.10.015.

51 P. Mukerjee and K. Mysels, *Critical Micelle Concentrations of Aqueous Surfactant Systems*, Office of Standard Reference Data, National Bureau of Standards, 1971.

52 K. L. Armbrust, Pesticide hydroxyl radical rate constants: Measurements and estimates of their importance in

aquatic environments, *Environ. Toxicol. Chem.*, 2000, **19**, 2175–2180, DOI: 10.1002/etc.5620190905.

53 X. Jin, S. Peldszus and P. M. Huck, Reaction kinetics of selected micropollutants in ozonation and advanced oxidation processes, *Water Res.*, 2012, **46**, 6519–6530, DOI: 10.1016/j.watres.2012.09.026.

54 V. Riffault, T. Gierczak, J. B. Burkholder and A. R. Ravishankara, Quantum yields for OH production in the photodissociation of HNO_3 at 248 and 308 nm and H_2O_2 at 308 and 320 nm, *Phys. Chem. Chem. Phys.*, 2006, **8**, 1079, DOI: 10.1039/b513760h.

55 J. Michalowski, P. Halaburda and A. Kojlo, Determination of humic acid in natural waters by flow injection analysis with chemiluminescence detection, *Anal. Chim. Acta*, 2001, 143–148, DOI: 10.1016/S0003-2670(00)01368-4.

56 J. J. Werner, K. McNeill and W. A. Arnold, Environmental photodegradation of mefenamic acid, *Chemosphere*, 2005, **58**, 1339–1346, DOI: 10.1016/j.chemosphere.2004.10.004.

57 S. Halladja, A. Amine-Khodja, A. ter Halle, A. Boulkamh and C. Richard, Photolysis of fluometuron in the presence of natural water constituents, *Chemosphere*, 2007, **69**, 1647–1654, DOI: 10.1016/j.chemosphere.2007.05.035.

58 R. P. Schwarzenbach, P. M. Gschwend and D. M. Imboden, *Environmental Organic Chemistry*, John Wiley and Sons, Hoboken, 2nd edn, 2003.

59 M. Elazzouzi, M. Mekkaoui, S. Zaza, M. El Madani, A. Zrineh and J. M. Chovelon, Abiotic degradation of imazethapyr in aqueous solution, *J. Environ. Sci. Health, Part B*, 2002, **37**, 445–451, DOI: 10.1081/PFC-120014874.

60 M. Ramezani, D. P. Oliver, R. S. Kookana, G. Gill and C. Preston, Abiotic degradation (photodegradation and hydrolysis) of imidazolinone herbicides, *J. Environ. Sci. Health, Part B*, 2008, **43**, 105–112, DOI: 10.1080/03601230701794968.

61 A. Latifoglu and M. D. Gurol, The effect of humic acids on nitrobenzene oxidation by ozonation and O_3/UV processes, *Water Res.*, 2003, **37**, 1879–1889, DOI: 10.1016/S0043-1354(02)00583-3.

62 M. Elazzouzi, A. Bensaoud, A. Bouhaouss, S. Guittonneau, A. Dahchour, P. Meallier and A. Piccolo, Photodegradation of imazapyr in the presence of humic substances, *Fresenius Environ. Bull.*, 1999, **8**, 478–485.

63 *Soil Survey of Nicollet County*, Department of Agriculture, Soil Conservation Service, Minnesota, United States, 1994.

64 O. Sakaliene, S. K. Papiernik, W. C. Koskinen and K. A. Spokas, Sorption and predicted mobility of herbicides in Baltic soils, *J. Environ. Sci. Health, Part B*, 2007, **42**, 641–647, DOI: 10.1080/03601230701465601.

65 R. M. Johnson and J. T. Sims, Influence of surface and subsoil properties on herbicide sorption by Atlantic Coastal Plain soils, *Soil Sci.*, 1994, **155**, 339–348.

66 M. Sleiman, P. de Sainte Claire and C. Richard, Heterogeneous Photochemistry of Agrochemicals at the Leaf Surface: A Case Study of Plant Activator Acibenzolar-*S*-methyl, *J. Agric. Food Chem.*, 2017, **65**, 7653–7660, DOI: 10.1021/acs.jafc.7b02622.

67 A. S. Trivella, S. Monadjemi, D. R. Worrall, I. Kirkpatrick, E. Arzoumanian and C. Richard, Perinaphthenone phototransformation in a model of leaf epicuticular waxes, *J. Photochem. Photobiol., B*, 2014, **130**, 93–101, DOI: 10.1016/j.jphotobiol.2013.10.009.

68 S. Monadjemi, A. ter Halle and C. Richard, Reactivity of cycloxydim toward singlet oxygen in solution and on wax film, *Chemosphere*, 2012, **89**, 269–273, DOI: 10.1016/j.chemosphere.2012.04.035.

69 L. Su, J. D. Sivey and N. Dai, Emerging investigator series: sunlight photolysis of 2,4-D herbicides in systems simulating leaf surfaces, *Environ. Sci.: Processes Impacts*, 2018, **20**, 1123–1135, DOI: 10.1039/C8EM00186C.

70 N. Schippers and W. Schwack, Photochemistry of imidacloprid in model systems, *J. Agric. Food Chem.*, 2008, **56**, 8023–8029, DOI: 10.1021/jf801251u.

71 G. Bianchi, P. Avato and F. Salamini, Surface waxes from grain, leaves, and husks of maize (*Zea mays* L.), *Cereal Chem.*, 1984, **61**, 45–47.

72 K. S. Kim, S. H. Park, D. K. Kim and M. A. Jenks, Influence of Water Deficit on Leaf Cuticular Waxes of Soybean (*Glycine max* [L.] Merr.), *Int. J. Plant Sci.*, 2007, **168**, 307–316, DOI: 10.1086/510496.

73 P. Cabras, A. Angioni, V. L. Garau, M. Melis, F. M. Pirisi and E. V. Minelli, Effect of epicuticular waxes of fruits on the photodegradation of fenthion, *J. Agric. Food Chem.*, 1997, **45**, 3681–3683, DOI: 10.1021/jf970102h.

74 D. Lavieille, H. A. Ter, P.-O. Bussiere and C. Richard, Effect of a spreading adjuvant on mesotrione photolysis on wax films, *J. Agric. Food Chem.*, 2009, **57**, 9624–9628, DOI: 10.1021/jf901996d.

75 E. L. Schymanski, J. Jeon, R. Gulde, K. Fenner, M. Ruff, H. P. Singer and J. Hollender, Identifying Small Molecules via High Resolution Mass Spectrometry: Communicating Confidence, *Environ. Sci. Technol.*, 2014, **48**, 2097–2098, DOI: 10.1021/es5002105.

